Bonn potential model at finite temperature

Song Gao and Yi-Jun Zhang
Department of Physics, Fudan University, Shanghai 200433, People's Republic of China

Ru-Keng Su
China Center of Advance Science and Technology (World Laboratory), P.O. Box 8730, Beijing 100080, People's Republic of China and Department of Physics, Fudan University, Shanghai 200433, People's Republic of China

(Received 17 July 1995)

By using the thermofield dynamics, we have calculated the effective coupling of nucleon-nucleon mesons by summing the three-lines vertices and the masses of nucleon and mesons by summing the corresponding self-energy diagrams of the Bonn potential model at finite temperature. Through the temperature dependence of effective couplings and the screening masses, we have extended the Bonn potential to finite temperature.

PACS number(s): 21.30.Fe, 11.10.Wx, 13.75.Cs

The Bonn potential [1] is one of the very successful potentials in nuclear physics. It provides a nice fit to nucleon-nucleon (NN) phase shifts and deuteron properties and is widely in use [1,2]. For studying physics under extreme condition of high temperature and/or high density, it is essential to extend the Bonn potential to finite temperature. This is the purpose of this paper.

The Bonn potential model is a boson-exchange model. The intermediate bosons in this model are π, σ, η, δ, ω, and ρ mesons which provide the long-range and intermediate-range as well as the short-range force for NN and $N\Delta$ interactions. For simplicity, we neglect the Δ resonance here. The interaction Lagrangian for the Bonn potential model is

$$\mathscr{L}_I=\mathscr{L}_{\rm ps}+\mathscr{L}_s+\mathscr{L}_v\,,$$

$$\mathscr{L}_{\rm ps}=-g_{\rm ps}\bar{\psi}i\gamma_5\psi\varphi,\quad \mathscr{L}_s=g_s\bar{\psi}\psi\phi, \tag{1}$$

$$\mathscr{L}_v=-g_v\bar{\psi}\gamma^\mu\psi V_\mu-\frac{f_v}{4m_N}\bar{\psi}\sigma^{\mu\nu}\psi(\partial_\mu V_\nu-\partial_\nu V_\mu),$$

where φ, ϕ, and V_μ are the pseudoscalar (π,η), scalar (σ,δ), and vector (ω,ρ) bosons, respectively, and m_N is the nucleon mass in vacuum.

We use the thermofield dynamics (TFD) [3] to extend the Bonn potential to finite temperature. In order to investigate the NN potential due to various meson exchanges, as in our previous studies [4–7], we calculate the three-line vertices correction [Fig. 1(a)] which will lead to the temperature dependence of $NN\alpha$ $(\alpha=\pi,\eta,\sigma,\delta,\omega,\rho)$ effective coupling, and the vacuum polarization [Fig. 1(b)] which will lead to the temperature dependence of the masses of mesons and nucleons, and then use the temperature-dependent effective coupling and masses to study the Bonn potential. In the framework of TFD, the thermal propagator has 2×2 matrix structure, but only the 1-1 component refers to the physical field [3]. The calculations are very complicated; hereafter we show the final result and some examples only.

1. Vertices correction. Each effective coupling of $NN\alpha$ includes six diagrams, because the exchanging mesons can be itself and five other mesons. For example, the effective coupling of a NN pseudoscalar meson due to the exchange of a pseudoscalar meson is

$$g_{\rm ps}\Lambda^{\rm ps}_{\rm ps}\gamma_5\tau_k=i\int\frac{d^4k}{(2\pi)^4}(g_{\rm ps}\gamma_5\tau_i)\Delta^{11}(p'-k)\times(g_{\rm ps}\gamma_5\tau_k)\Delta^{11}(p-k)(g_{\rm ps}\gamma_5\tau_i)D^{11}_{\rm ps}(k), \tag{2}$$

where

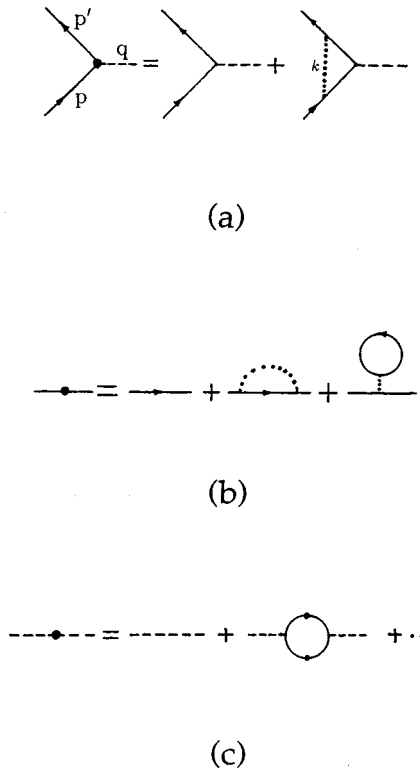

FIG. 1. Feynman diagrams. (a) The three-line vertices; the solid lines denote nucleons, the dashed lines for the corresponding mesons, and the dotted lines for all mesons. (b) Self-energy diagrams for the nucleon. (c) Self-energy diagrams for the meson.

$$\Delta^{11}(k)=(\not{k}+m_N)\left[\frac{1}{k^2-m_N^2+i\epsilon}+2\pi i n_F(k)\,\delta(k^2-m_N^2)\right], \tag{3}$$

$$D^{11}(k)=\frac{1}{k^2-m_\alpha^2+i\epsilon}-2\pi i n_B(k)\,\delta(k^2-m_\alpha^2), \tag{4}$$

are the 1-1 component propagators for fermions and bosons, respectively [3,6,7]. Substituting Eqs. (3) and (4) into Eq. (2), we can prove that Eq. (2) can be separated into two parts: the zero-temperature part and the temperature-dependent part. The contribution of the zero-temperature part can be treated by introducing a form factor as in Ref. [1], and the temperature-dependent part is

$$\Lambda_{\rm ps}^{\rm ps}(T)=-g_{\rm ps}^2\int\frac{d^4k}{(2\pi)^3}\frac{k^2}{[(p'-k)^2-m_N^2][(p-k)^2-m_N^2]}\,\delta(k^2-m_{\rm ps}^2)n_B(k)+g_{\rm ps}^2\int\frac{d^4k}{(2\pi)^3}\frac{k^2}{[(p-k)^2-m_N^2](k^2-m_{ps}^2)}$$
$$\times\,\delta[(p'-k)^2-m_N^2]n_F(p'-k)+g_{\rm ps}^2\int\frac{d^4k}{(2\pi)^3}\frac{k^2}{[(p'-k)^2-m_N^2](k^2-m_{\rm ps}^2)}\,\delta[(p-k)^2-m_N^2]n_F(p-k). \tag{5}$$

The vertex correction of pseudoscalar mesons due to the exchange of scalar mesons or vector mesons can be calculated similarly. The total vertices correction of pseudoscalar mesons at finite temperature is

$$\Lambda_{\rm ps}(T)=\Lambda_{\rm ps}^{\rm ps}(T)+\Lambda_{\rm ps}^{s}(T)+\Lambda_{ps}^{v}(T) \tag{6}$$

and the effective coupling of the pseudoscalar meson is

$$g_{\rm ps}^*(T)=g_{\rm ps}[1+\Lambda_{\rm ps}(T)]. \tag{7}$$

The calculations of the temperature-dependent effective couplings for other mesons are analogous to that for the pseudoscalar meson. But for the ρNN coupling, there are two coupling constants g_ρ and f_ρ which correspond to the vector coupling and the tensor coupling, respectively.

2. Self-energy corrections. According to the Feynman rules of TFD, the in-medium nucleon mass m_N^* can be found by summing the self-energy diagrams [Fig. 1(b)] where the dashed lines denote the corresponding six mesons. The self-energy corrections of mesons can be obtained by summing the corresponding self-energy diagrams of mesons [Fig. 1(c)]. For example, the self-energy of pseudoscalar mesons is

$$\Pi_{\rm ps}(q)=ig_{\rm ps}^2\int\frac{d^4k}{(2\pi)^4}{\rm Tr}[\gamma_5\tau_i\Delta^{11}(k)\gamma_5\tau_j\Delta^{11}(k+q)]. \tag{8}$$

Substituting the nucleon propagator into Eq. (8), we can separate $\Pi_{\rm ps}(q)$ into two parts: $\Pi_{\rm ps}(q)=\Pi_{\rm ps}^F(q)+\Pi_{\rm ps}(q,T)$. The last term depends on temperature explicitly, and the first term $\Pi_{\rm ps}^F(q)$ depends on m_N^*. Obviously, $\Pi_{\rm ps}^F(q)$ involves divergent integrals and also depends on temperature through m_N^*. These divergences may be rendered finite by a regularization procedure as in Refs. [8,9], and the finite parts are called the vacuum fluctuation (VF)

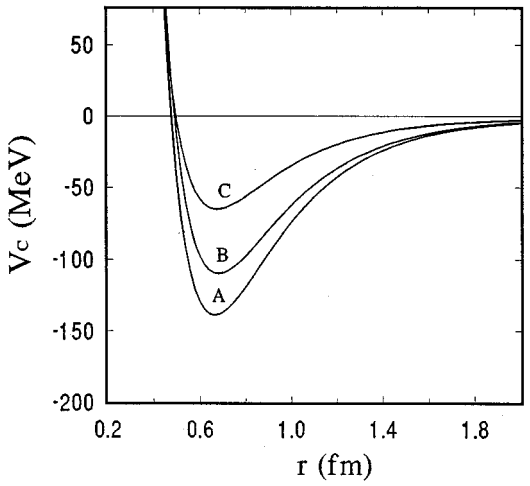

FIG. 2. The central potential at different temperatures. A: $T=0$; B: $T=100$ MeV; C: $T=150$ MeV.

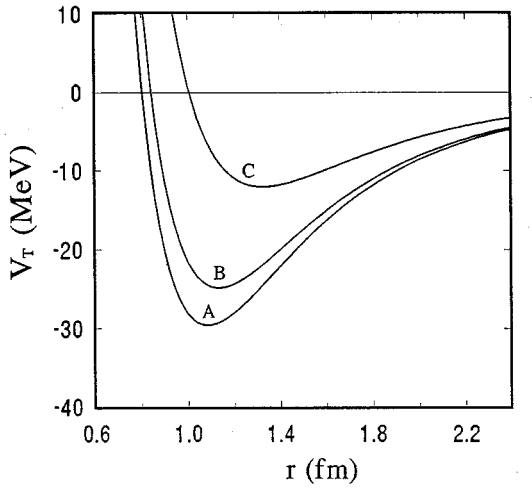

FIG. 3. The tensor potential at different temperatures. A: $T=0$; B: $T=100$ MeV; C: $T=150$ MeV.

correction. After the above treatment we find that the VF part of the self-energy of a π meson, for example, is

$$\Pi_\pi^F(q)=-\frac{g_\pi^2}{2\pi^2}\left\{m_N^2-m_N^{*2}-2(m_N-m_N^*)^2+\tfrac{1}{6}(q^2-m_\pi^2)+\int_0^1 dx[m_N^{*2}-3q^2x(1-x)]\times\ln\left[\frac{m_N^{*2}-q^2x(1-x)}{m_N^2-q^2x(1-x)}\right]\right\}. \tag{9}$$

$\Pi_{\rm ps}(q,T)$ can be calculated as in Refs. [6,11] directly.

The screening masses of mesons which represent the inverse Debye screening length and imply the long-distance corrections are defined as in Refs. [10,11]:

$$m_\alpha^s=[m_\alpha^2+\Pi_\alpha(0,\vec{q}\to 0;T,\rho)]^{1/2}(\alpha=\pi,\sigma,\eta,\delta,\omega,\rho). \tag{10}$$

3. Bonn potential at finite temperature. The *NN* potential due to the one-boson exchange can be found by summing the exchange amplitude of certain bosons with given screening masses and effective couplings. Following a treatment similar to our previous work [4–7,11], we finally obtain the *NN* potential at finite temperature for the Bonn potential model as

$$V_{\rm Bonn}(r)=\sum_\alpha V_\alpha(r), \tag{11}$$

$$V_{\rm ps}(r)=H_{\rm ps}\frac{g_{\rm ps}^{*2}}{4\pi}\frac{m_{\rm ps}^{s3}}{12m_N^2}[Z(x_{\rm ps})S_{12}+Y(x_{\rm ps})(\vec{\sigma}_1\cdot\vec{\sigma}_2)], \tag{12}$$

$$V_s(r)=-H_s\frac{g_s^{*2}}{4\pi}m_s^s\left[\left(1-\frac{m_s^{s2}}{4m_N^2}\right)Y(x_s)-\frac{m_s^{s2}}{2m_N^2}\vec{S}\cdot\vec{L}\frac{1}{x_s}\frac{d}{dx_s}Y(x_s)\right], \tag{13}$$

$$\begin{aligned}V_v(r)=&\frac{H_{vL}}{4\pi}m_{vL}^s\left\{g_v^{*2}\left[\left(1+\frac{m_{vL}^{s2}}{4m_N^2}\right)Y(x_{vL})-\tfrac{1}{2}Z_1(x_{vL})\vec{L}\cdot\vec{S}\right]+\frac{1}{2}g_v^*f_v^*\left[\left(\frac{m_{vL}^s}{m_N}\right)^2Y(x_{vL})-2Z_1(x_{vL})\vec{L}\cdot\vec{S}\right]\right\}\\&+\frac{H_{vT}}{4\pi}m_{vT}^s\left\{g_v^{*2}\left[\frac{m_{vT}^{s2}}{4m_N^2}\left(1-\frac{m_{vT}^{s2}}{16m_N^2}\right)Y(x_{vT})-\left(1-\frac{m_{vT}^{s2}}{16m_N^2}\right)Z_1(x_{vT})\vec{L}\cdot\vec{S}+\frac{1}{6}\left(\frac{m_{vT}^s}{m_N}\right)^2Y(x_{vT})(\vec{\sigma}_1\cdot\vec{\sigma}_2)-\tfrac{1}{12}Z(x_{vT})S_{12}\right]\right.\\&\left.+g_v^*f_v^*\left[\frac{1}{3}\left(\frac{m_{vT}^s}{m_N}\right)^2Y(x_{vT})(\vec{\sigma}_1\cdot\vec{\sigma}_2)-Z_1(x_{vT})\vec{L}\cdot\vec{S}-\tfrac{1}{6}Z(x_{vT})S_{12}\right]+\frac{f_v^{*2}}{6}\left[\left(\frac{m_{vT}^s}{m_N}\right)^2Y(x_{vT})(\vec{\sigma}_1\cdot\vec{\sigma}_2)-\tfrac{1}{2}Z(x_{vT})S_{12}\right]\right\},\end{aligned} \tag{14}$$

where $\alpha=\pi,\eta,\sigma,\delta,\rho,\omega$, and $H_{\rm ps}$, H_{vL}, H_s, and H_{vT} are some convergent integrals [7,11]. The contributions from the isovector bosons π, δ, and ρ will multiply a factor of $\vec{\tau}_1\cdot\vec{\tau}_2$ to the corresponding equations (12), (13), and (14). The $x_i=m_i^s r$, $Y(x_i)$, $Z_1(x_i)$, $Z(x_i)$, and S_{12} are defined as in Ref. [1].

The Bonn potential can be separated into different components as

$$V_\alpha(r)=V_C(r)+V_T(r)S_{12}+V_{LS}(r)\vec{L}\cdot\vec{S}, \tag{15}$$

where $V_C(r)$, $V_T(r)$, and $V_{LS}(r)$ are, respectively, the central, tensor, and spin-orbit potentials.

The numerical results of the Bonn potential at finite temperature are shown in Figs. 2–4, where the parameters have been chosen as in Ref. [1]. The central potential curves for different temperatures $k_BT=0$ (A), 100 (B), and 150 (C) MeV are shown in Fig. 2. From Fig. 2, we find that the potential well of $V_C(r)$ becomes shallower as the temperature increases. The tensor potential curves for different temperature are shown in Fig. 3. As the temperature increases, the zero of the tensor force is shifted toward the large r region, and the tensor force is weaker in the outer region. This result is in agreement with the in-medium tensor force [12]. Figure 4 shows the curves of the spin-orbit $V_{LS}(r)$ for various temperatures; the absolute value of the spin-orbit potential $|V_{LS}(r)|$ increases as temperature increases, but

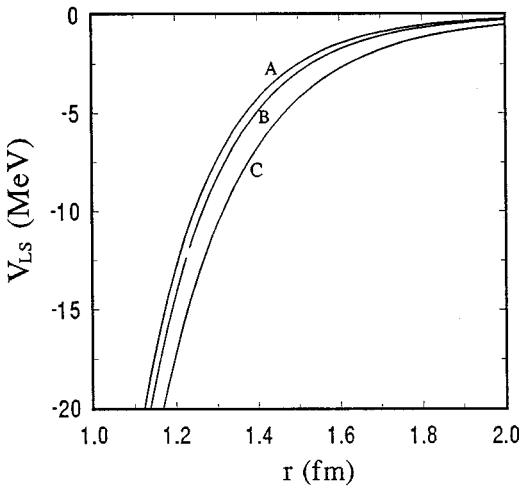

FIG. 4. The spin-orbit potential at different temperatures. A: $T=0$; B: $T=100$ MeV; C: $T=150$ MeV.

$V_{LS}(r)$ is not sensitive to temperature. The above result is of course reasonable because the temperature plays a ''repulsive'' role.

Since the Bonn potential is the meson-exchange potential, the above derived temperature dependence is valid only at the temperature region below the chiral and/or deconfining critical temperature. If one wants to discuss the nuclear force based on the quark model, in particular, on QCD, some corrections, for example, the cutoff in the meson-nucleon vertex form factors, must be added to the Bonn potential [13].

By using our temperature-dependent Bonn potential, we can discuss the equation of state, the temperature dependence of the saturation point of nuclear matter, and others. Work in this topic is in progress.

This work was supported in part by NNSF of China.

[1] R. Machleidt, Adv. Nucl. Phys. **19**, 189 (1989); R. Machleidt, K. Holinde, and Ch. Elster, Phys. Rep. **149**, 1 (1987).
[2] K. Holinde and A. W. Thomas, Phys. Rev. C **42**, R1195 (1990).
[3] H. Umezawa, H. Matsumoto, and M. Tachiki, *Thermo Field Dynamics and Condensed States* (North-Holland, Amsterdam, 1982); N. P. Landsman and Ch. G. van Weert, Phys. Rev. **145**, 141 (1987).
[4] R. K. Su and G. T. Zheng, J. Phys. G **16**, 203 (1990); R. K. Su, Z. X. Qian, and G. T. Zheng, *ibid.* **17**, 1785 (1991); R. K. Su, G. T. Zheng, and G. G. Siu, *ibid.* **19**, 79 (1993).
[5] Z. X. Qian, C. G. Su, and R. K. Su, Phys. Rev. C **47**, 877 (1993).
[6] S. Gao, Y. J. Zhang, and R. K. Su, Phys. Rev. C **52**, 380 (1995).
[7] R. K. Su, S. J. Yang, S. Gao, and P. K. N. Yu, J. Phys. G **20**, 1757 (1994); S. Gao, R. K. Su, and P. K. N. Yu, Phys. Rev. C **49**, 40 (1994).
[8] R. J. Furnstahle and C. J. Horowitz, Nucl. Phys. **A485**, 632 (1988).
[9] H. Shiomi and T. Hatsuda, Phys. Lett. B **334**, 281 (1994).
[10] C. Song, Phys. Rev. D **48**, 1875 (1993); **49**, 1556 (1994).
[11] S. Gao, Y. J. Zhang, and R. K. Su, J. Phys. G (in press); Nucl. Phys. A (in press).
[12] G. E. Brown and M. Rho, Phys. Lett. B **237**, 3 (1990).
[13] X. Shakin *et al.*, Brooklyn Report No. BCCNT 95/051/246, 1995.